ARCHIVES OF ACOUSTICS
9, 1-2, 181-190 (1984)

CARDIOVASCULAR DIAGNOSIS WITH FREQUENCY SPECTRAL ANALYSIS (FSA) AND CONTINUOUS WAVE DOPPLER (CWD)

MERRILL P. SPENCER

Institute of Applied Physiology and Medicine, Seattle, USA

This report reviews how the combined use of continuous wave Doppler ultrasound and frequency spectral analysis from the fast Fourier transform provides a useful means of finding and analysing non invasively a wide range of cardiovascular diagnostic information. Reliance is placed on the frequency resolution capability of CWD to follow increased velocities in arteries produced by arterial and cardiac value stenosis, valve regurgitations, congenital heart septal defects and arteriovenous shunts. The ability to detect turbulence energies simultaneously with high velocities "on line" with a video reproducable format improves and hastens the diagnosis.

Quantitation of stenotic lesion is possible in terms of effective lumen diameter and pressure drop produced by the blood flow. Cardiac output and changes in stroke volume can also be computed.

As Doppler ultrasonic equipment and examination techniques improve the range of Doppler detectable features of the circulatory system is expanding. The frequencies generated by the Doppler effect represent the velocity of blood streams in the heart, arteries and veins as well as motions of the cardiovascular structures. Blood velocity features from which diagnoses of abnormalities can be concluded include flow direction, acceleration, pulsatile waveform, as well as spectrum and spatial distribution of the flow streams. Ultrasonic frequencies from 2 to 10 MHz penetrate the body well and generate frequencies conveniently falling in the audible range allowing the use of the human hearing system as an analytical tool. This arrangement, when used with an understanding of hemodynamics, makes a remarkably cost-effective method for diagnosis of many cardiovascular disorders.

We have exploited the unlimited frequency resolution of CWD where the spatial resolution of pulsed wave Doppler (PWD) was not needed in disease diagnosis and quantitation. PWD is helpful where depth resolution is really

important but works best with 2 dimensional echography and it thus becomes less cost effective. CWD often provides more clear signals, safer power levels and easier location of diagnostic signals.

For documentation and study analogue tracings of selected components from the full spectrum of sounds generated has been widely used on available polygraphs to follow estimations of mean or maximum frequencies. These features, however, can be distorted by high energies produced by disease in the low frequency ranges. Though high pass filtering can eliminate these disturbances much information in the complete spectrum is lost from future analysis. The use of FSA from the fast Fourier transform (FFT) in video format [1] displays a much greater range of Doppler information than an analogue tracing assisting at the time of the patient examination and in future analysis [2]. The directional A and B quadrature signals of the Doppler equipment in the FFT analyses provides the equivalent of 256 band pass filters with a 10 ms updating time. The energies produced in each frequency band are color coded on a thermal scale with white representing the highest energies, red used for the lowest and with oranges and yellows representing the middle ranges. Black and white prints thus provide a gray scale with highest energies being darker. The maximum edge of the spectrum (f_{max}) has the same clinical usefulness desired of the analogue tracings to follow pulsatile contours, while preserving the lower frequency information representing velocity distributions within the vessel.

Normal laminar flow profiles in the internal and external carotid arteries are shown in Figs. 1 and 2. The differences in f_{max} contours are characteristic of the internal and external carotids. Higher diastolic f_{max} contours, when compared with the systolic peak f_{max}, reflects lower peripheral resistance in the brain than in the external carotid.

Fig. 3 illustrates the ability of FSA to simultaneously follow the pulse contours of f_{max} and display severe turbulence phenomena. The high velocity jet emerging from the stenotic arteries, represented by the high frequency (8 KHz) Doppler signals, produces lateral excursions in flow both towards and away from the probe resulting in high energy low frequency signals on either side of the zero reference. The analogue tracings of the zero crossing meter output are biased toward the lower frequencies and cannot follow the mean frequency in this situation. FSA can assist CWD to increase spatial resolution by displaying the superimposed spectra of two arteries lying in the ultrasonic beam (Fig. 4). The use of the CWD imaging technique [3, 4] also assists in specifying which branch at a bifurcatian is stenotic and which is nornal. CWD imaging of the carotid bifurcation is achieved by holding the probe in a mechanical arm fixing the angle of the ultrasound beam at 60° with the body axis. If the same angle is assumed for an artery running parallel to the body axis the frequency spectrum can be calibrated in m/s. For 5 MHz, in the case of Fig. 4, one kHz is equivalent to 0.3 m/s.

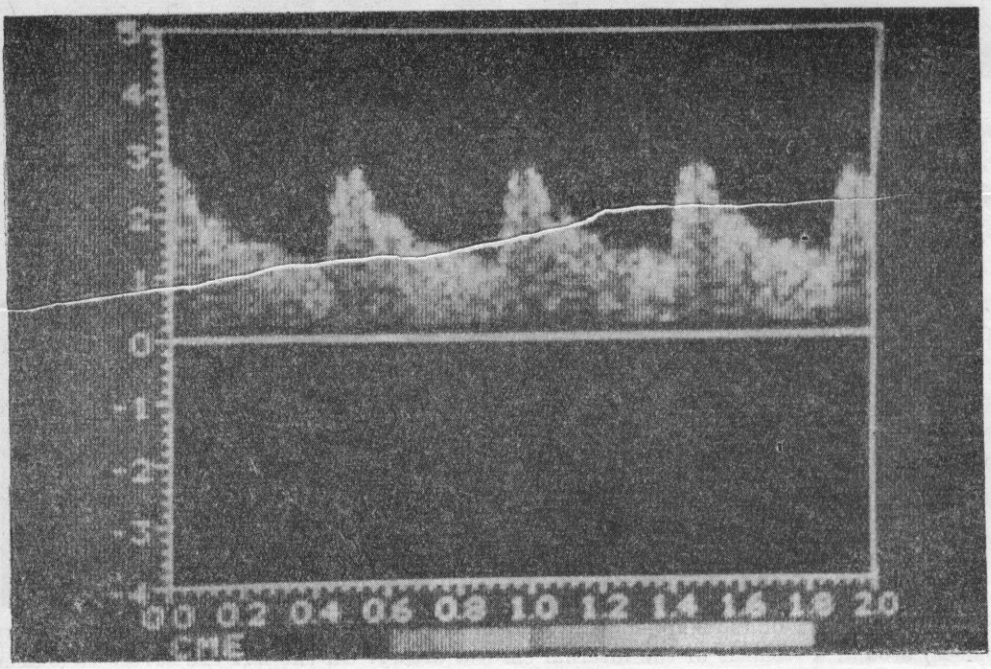

Fig. 1. FSA of Doppler frequencies detected in the normal internal carotid artery. The abcissa presents a 2 second sweep. The ordinate is calibrated in kHz with velocities away from the transducer represented above the zero line. Laminar flow with a blunt profile can be concluded from this display because of the concentration of energies near the upper edge of the spectrum (f_{max}). The high diastole and downsloping contours of f_{max} is characteristic of blood flow in arteries perfusing the brain

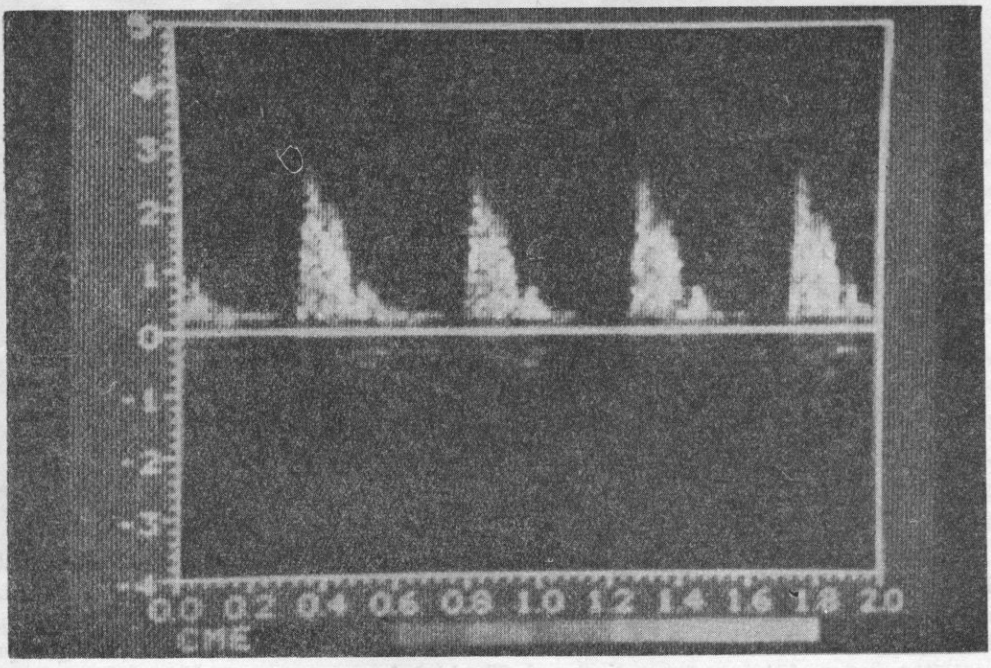

Fig. 2. FSA of Doppler signals in the normal external carotid artery. The probe beam angle is approximately 45° with the vessel as in Fig. 1. The frequency energies are rather evenly distributed across the spectrum indicating a more parabolic flow profile. The waveform is typical of the external carotid with lower diastolic velocities represented

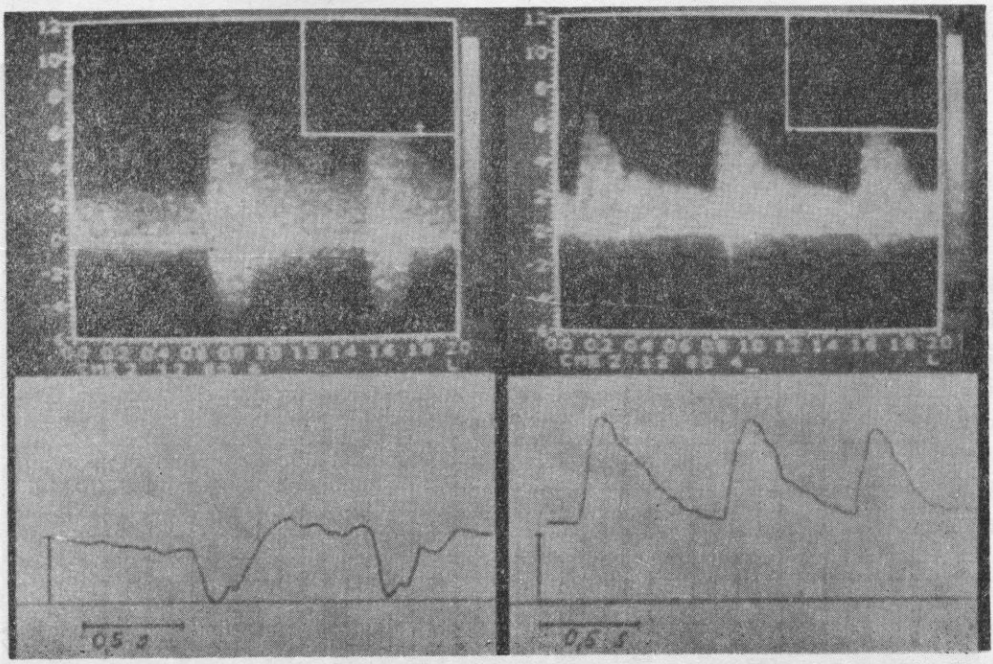

Fig. 3. Comparison of FSA (upper panels) with zero crossing meter analogue tracing (lower panels) around a stenosis of the internal carotid artery. On the left the severe turbulence produces strong dual directional energies in the lowest frequency ranges displayed on both sides of the zero reference causing the zero crossing output to decrease when, in fact, the maximum velocity is increasing. On the right where turbulences are not as strong the meter can follow the increased velocities

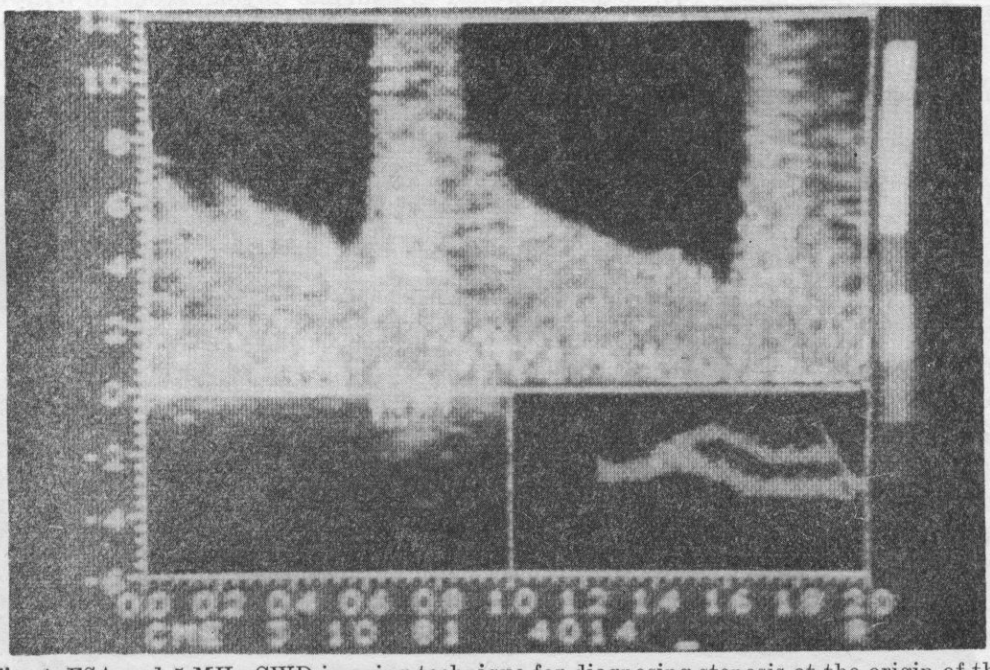

Fig. 4. FSA and 5 MHz CWD imaging technique for diagnosing stenosis at the origin of the internal carotid artery at its origin from the common carotid. A CWD image of the carotid bifurcation is seen in the lower right corner of the figure. The bright spot on the image represents the source of the spectrum displayed. The high frequency contour (> 12 kHz at peak systole), with a typical internal carotid contour, indicates stenosis of this artery while the superimposed external carotid spectrum, with only slightly elevated frequencies represents collateral flow velocities. Turbulence, associated with stenosis, is represented by the high systolic energies on both sides of the zero line

The maximum CWD frequency sound within a stenotic segment of the internal carotid artery can be used to estimate the degree of stenosis in terms of both stenosis diameter [5] (equivalent cross-sectional area) and the pressure drop produced [6] by the stenosis. Fig. 5 illustrates the relationship between peak systolic frequency and minimum diameter found in arteriographic examinations. The ability of CWD with FSA to predict the arteriographic diameter of the carotid is very good in the middle velocity range from 1.5 to 3.5 m/s.

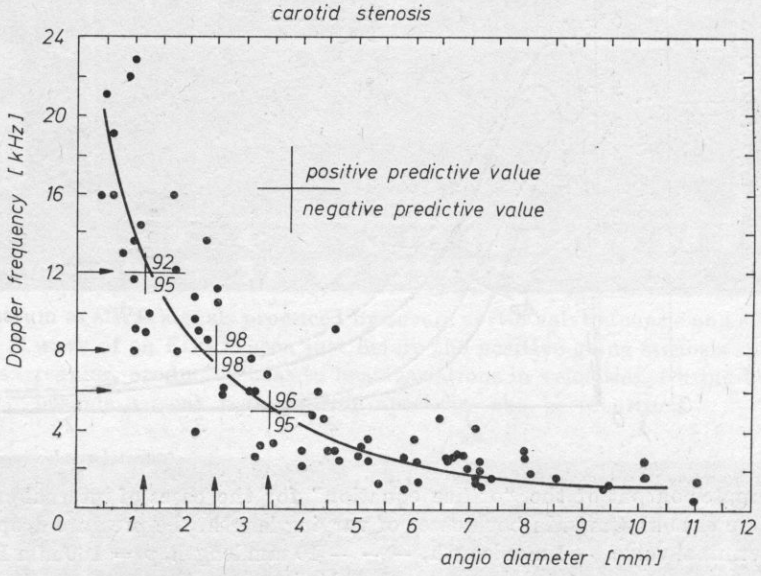

Fig. 5. Relationship found by clinical experience between the CWD peak systolic f_{max} and the angiographically determined diameter of 108 internal carotid arteries. One or both sides were stenotic. The predictive values are for accuracy limits set at ± 0.7 mm and ± 1 kHz (the limits of accuracy for both angiography and Doppler)

Mathematical modelling of the "orifice equation" is helpful in understanding the hemodynamics of stenosis. The total pressure drop (Δp) produced by a stenosis can be calculated by combining the three principle terms of Bernoulli, boundary effects, and Poiseuille [7]. Fig. 6 provides a computer solution output to such an equation for two cases of stenosis length showing how velocities v increase with increasing degrees of stenosis, as in the clinical data of Fig. 5, until the stenosis radius is less than 0.5 mm where velocities are diminishing to zero. Though the relationship between radius and both Δp and v is affected by stenosis length, the relationship between Δp and v is constant. For example, at a velocity of 4 m/s, in both cases, Δp reaches 1/2 of its terminal value. Also for all cases > 0.5 mm, where turbulence is quite apparent:

$$\Delta p\,[\text{mm Hg}] = 4v^2\,[\text{m/s}].$$

This simple relationship between Δp and v has been shown to hold for stenosis of heart valves and probably is correct for carotid artery stenosis. CWD combined with FSA provides a good method of applying these principles to compute an important hemodynamic parameter.

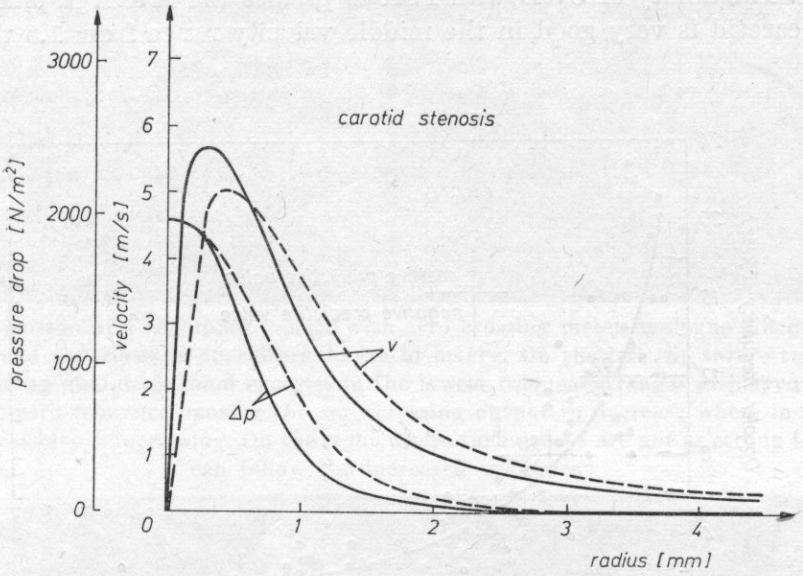

Fig. 6. Computer output of the "orifice equation" for the cases of internal carotid artery stenosis. Note that at 4 m/s, in both cases of varying length, the pressure drop reaches one half of its terminal value. — 1 mm length, — — — 10 mm length, p = 160 mm Hg, R_p = 0.3 mm Hg/ml/min

Cardiac diagnoses, with combined CWD and FSA, include stenosis and regurgitation of the valves, congenital septal defects as well as aortic coarctation and patent ductus arteriosus [8]. The diagnosis is made from the contour and timing of f_{max} which is increased above normal to follow elevated blood velocities through these orifices. Strong cardiac motion signals and severe turbulence energies must be attenuated by means of a high pass filter. A few examples of CWD spectra that occur in aquired valve lessions will illustrate the usefulness of the technique. Fig. 7 demonstrates the high velocity signals of aortic valve stenosis in a patient when directing a 2.5 MHz CW ultrasound beam from the precordium apical region. Since this probe position produced the highest Doppler frequencies we can assume the beam was to be in line with the jet stream allowing the ordinate to be transposed to m/s. The pressure drop accross the stenotic orifice can the be calculated from the equation previously given.

CWD with FSA is especially sensitive to valve regurgitations and probably is more sensitive than standard contrast cineangiography. Slight aortic

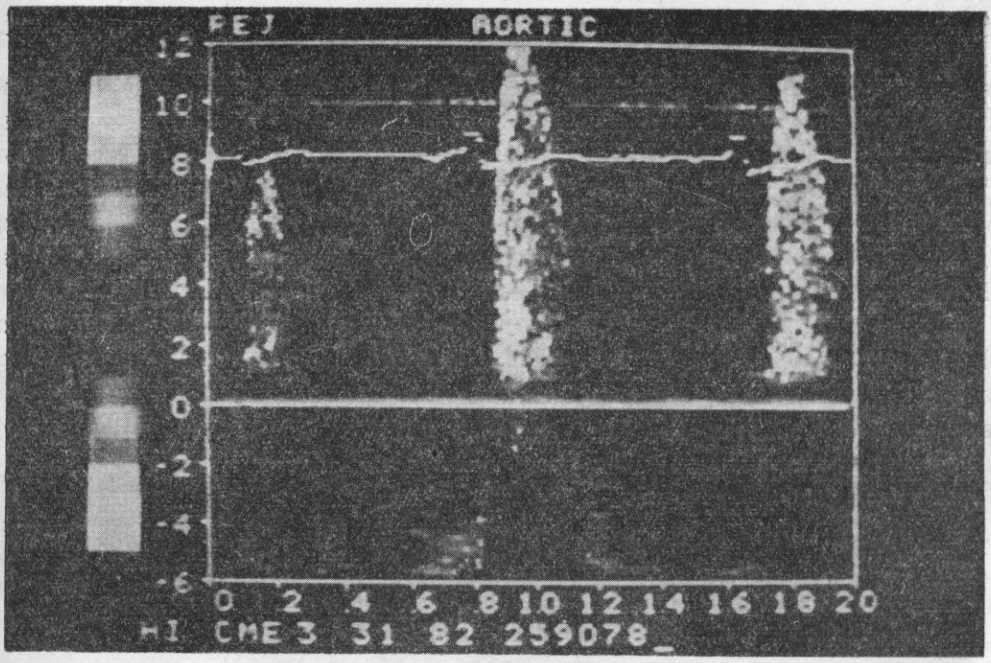

Fig. 7. Spectrum of CWD signals produced by severe aortic valve stenosis and slight regurgitation. The *R* wave of an ECG is seen just before the positive going stenosis spectrum. The heart rate is irregular, producing beat to beat variations in velocities. During both diastolic periods a weak regurgitation spectrum can be identified

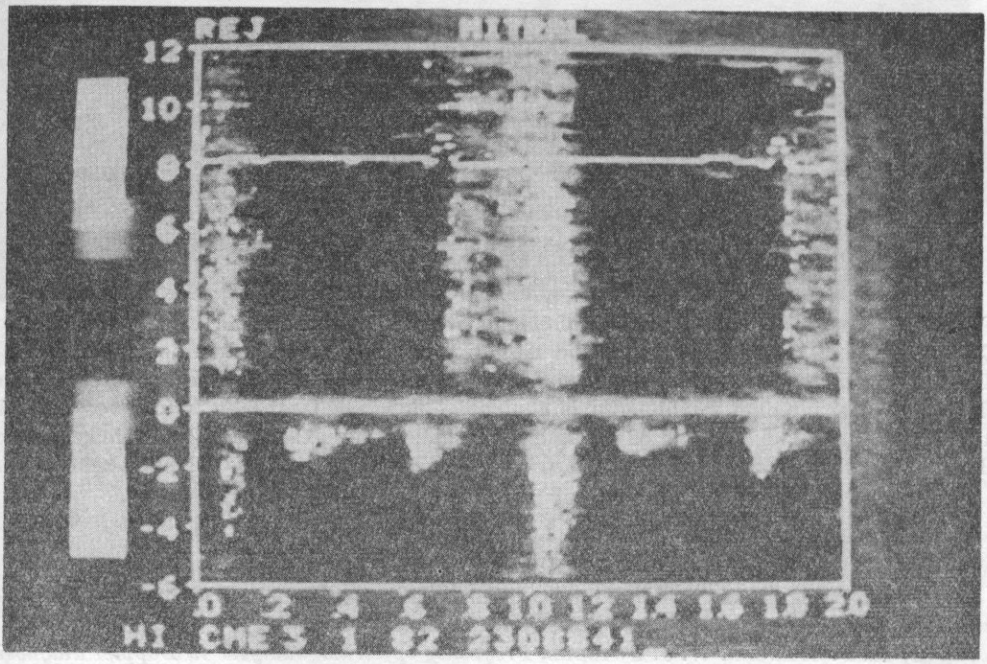

Fig. 8. Mitral valve prolapse regurgitation spectrum of CWD. Note accentuation of jet in late systole with dual directional turbulence represented

regurgitation is represented in Fig. 7 by the spectrum seen below the zero line during diastole. Fig. 8 illustrates the regurgitant signals of mitral valve prolapse where accentuation of the lower ranges of the spectrum occurs in late systole. The leak becomes large enough to produce strong turbulence signals displayed both above to below the zero line. Normal mitral inflow signals are seen during diastole below the zero line indicating no stenosis of the valve is present and also the leak is not severe enough to noticably increase inflow velocities.

Changes in stroke volume of the left ventricle can also be followed from the systolic velocity contours found in the ascending aorta and stroke volume and cardiac output may be calculated when the diameter of the ascending aorta is known from echocardiographic angiographically recorded sources [9] (Fig. 9).

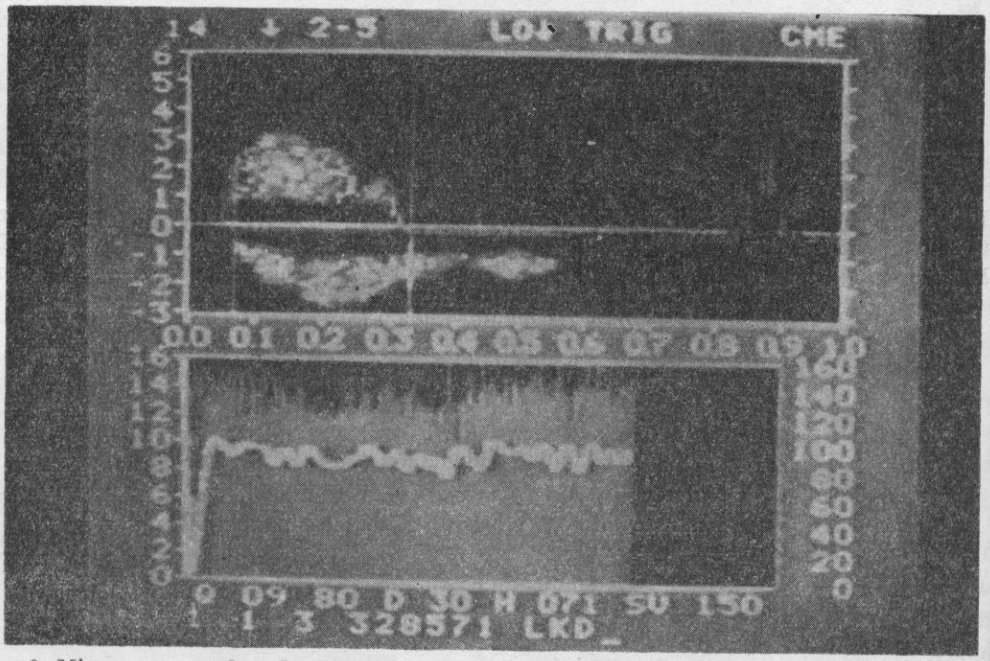

Fig. 9. Microprocessor based method of calculating stroke volume and cardiac output from CWD spectra of velocities found in the ascending aorta of a normal subject. The probe is directed from the suprasternal notch and only the spectrum of velocities directed towards the probe (positive ones in this case) is analysed. The mean frequency is followed near the upper edge, f_{max}. The diameter of the ascending aorta is set in each case. In the lower section the trend of the cardiac output from heart rate and stroke volume is followed beat to beat

References

[1] M. P. Spencer, R. E. Hileman, *Cardiac diagnosis with directional CW Doppler and FFT color video spectral display*, J. Ultra. Med, **1**, 117 (1982).

[2] M. P. Spencer, W. J. Zwiebel, *Frequency spectrum analysis in Doppler diagnosis*, chapter 8, in: *Introduction to vascular ultrasonography*, W. J. Zwiebel (ed.), Grune Stratton, New York 1982.

[3] M. P. SPENCER, J. M. REID, *Cerebrovascular evaluation with Doppler ultrasound,* Martinus Nijhoff, The Hague-Boston-London, 1981.

[4] M. P. SPENCER, J. M. REID, D. L. DAVIS, P. S. PAULSON, *Cervical carotid imaging with a continuous wave Doppler flowmeter,* Stroke, **5**, 145-154 (1974).

[5] M. P. SPENCER, J. M. REID, *Quantitation of carotid stenosis with continuous wave (C-W) Doppler ultrasound,* Stroke, **10**, 326-330 (1979).

[6] J. HOLEN, R. AASLID, K. LANDMARK, S. SIMONSEN, *Determination of pressure gradient in mitral stenosis with a non-invasive ultrasound Doppler technique,* Acta Med. Scand., **199**, 455 (1976).

[7] M. P. SPENCER, T. ARTS, *Hemodynamic principles for cardiac Doppler diagnosis,* chapter 14, in: *Cardiac Doppler diagnosis,* M. P. SPENCER (ed.), Martinus Nijhoff, The Hague, 1983.

[8] L. HATLE, B. ANGELSEN, *Doppler ultrasound in cardiology. Physical principles and clinical applications,* Lea and Febiger, 1982.

[9] L. L. HUNTSMAN, E. GAMS, C. C. JOHNSON, E. FAIRBANKS, *Transcutaneous determination as aortic blood flow velocities in man,* Am. Heart J., **89**, 609 (1975).